LINC

Learning about Interacting Networks in Climate

Marie Curie Initial Training Networks (ITN)

FP7- PEOPLE - 2011- ITN

Grant Agreement No. 289447

WorkPackage WP5: *Tipping points of the climate system*

Deliverable D5.5
Report on indicators for tipping points from Lagrangian and discretisation networks

Emilio Hernández-García, UIB

Víctor Rodríguez-Méndez, UIB

Enrico Ser-Giacomi, UIB

Release date: 28 August 2015

Status: PU

EXECUTIVE SUMMARY

The main objective of Workpackage 5 of the LINC project ``Tipping Points in the Climate System" is to find indicators, based on network theory, of regime changes in the climatic system, and also quantities that can provide early warnings of them.

Most of the climatic networks constructed within the LINC project are based on statistical relationships (correlations, mutual information) among different geographic regions represented by the network nodes. But one of the tasks of Workpackage 1 was the development of an alternative representation of climatic processes, namely to represent with the network links mass exchange --transport of air or water-- among different regions. The study of these novel Lagrangian or Flow Networks has been the subject of previous deliverables and publications.

In this deliverable four network indicators, which were useful to identify and to anticipate tipping points in climatic networks constructed from correlations, are applied to a flow network to assess their performance there. The chosen flow network is a kinematic flow model that mimics the topology of the atmospheric circulations during blocking events such as the one occurring over Eastern Europe and Russia in summer 2010.

The result is that three of the tested indicators are good indicators of the flow regime changes. In addition one of them, the average clustering, seems to provide an early warning of the tipping point, so that it is a promising quantity to be analyzed further for its anticipating potential.

Deliverable Identification Sheet

Grant Agreement No.	**PITN-GA-2011-289447**
Acronym	**LINC**
Full title	**Learning about Interacting Networks in Climate**
Project URL	http://climatelinc.eu/
EU Project Officer	Athina ZAMPARA

Deliverable	**D5.5 Report on indicators for tipping points from Lagrangian and discretisation networks**
Work package	**WP5 Tipping points of the climate system**

Date of delivery	**Contractual**	M 45	**Actual**	28-August-2015
Status	version. 1.00		final ☑ draft □	
Nature	Prototype □ Report ☑ Dissemination □			
Dissemination Level	Public √ Consortium ☐			

Authors (Partner)	Emilio Hernández-García (UIB), Víctor Rodríguez-Méndez (UIB), Enrico Ser-Giacomi (UIB)			
Responsible Author	**Emilio Hernández-García**		**Email**	emilio@ifisc.uib-csic.es
	Partner	UIB	**Phone**	+34 971171307

Abstract (for dissemination)	This deliverable examines the performance of four network indicators to identify and to anticipate the occurrence of transitions among flow regimes in geophysical flows. A kinematic flow model, capturing characteristics of atmospheric circulations occurring during a blocking event, is analysed with network quantifiers. Three of them are shown to be good indicators of the tipping point, or to anticipate it.	
Keywords	Tipping points, early warnings, flow networks, fluid transport, regime changes	

Version Log			
Issue Date	**Rev No.**	**Author**	**Change(s)**
28-8-2015	001	E. Hernández-García	Final document

Contents

EXECUTIVE SUMMARY **ii**

CONTENTS **iv**

1 Introduction **1**

2 Model and its relationship with atmospheric circulation **1**

3 Cross-flow transition **6**

4 Network indicators and discussion **6**

REFERENCES **9**

1 Introduction

Workpackage 5 of the LINC project was devoted to the development of techniques based on network theory to identify and to predict the approach of the climate system to *tipping points* (i.e. abrupt transitions to new climatic regimes). In the work summarized in Deliverables 5.2-5.4 and in the associated publications (Van Der Mheen et al., 2013; Tirabassi et al., 2014; Feng et al., 2014) these techniques have been established and demonstrated for climate networks constructed from correlations (or other statistical dependence measures) between climatic variables at different geographical locations. On the other hand, one of the tasks of Workpackage 1 was the construction of climate networks from an alternative point of view, namely characterizing the transport of air and water masses between different parts of the Earth (flow transport or Lagrangian networks). Thus, it is natural to explore also the feasibility of using these alternative network representations to anticipate transitions. This is the subject of this deliverable.

Because of its explorative character, the research summarized here has been focussed on a kinematic flow model rather than in an observed or modeled geophysical flow. In Section 2 we define the flow model and its relationship with example flow configurations in the atmosphere, extracted from the blocking event occurring over Eastern Europe and Russia in Summer 2010 (Ser-Giacomi et al., 2015*c*). In Section 3 we show that the model system has a cross-flow transition similar to the changes in the atmospheric regimes. Network indicators of the transition are discussed in Sect. 4.

2 Model and its relationship with atmospheric circulation

We want to explore the possibility to use topological characteristics of flow networks as indicators of transitions occurring in the flow system. The type of transitions we want to explore are illustrated in Fig. 1. They show *optimal paths* followed by air parcels during a blocking event occurring in July 2010. Black circles are the trajectories starting location (lateral initial spread of 1.5^o). Details on the data used to compute the trajectories, their dates, the meaning of the optimality condition and of the color code are explained in Ser-Giacomi et al. (2015*c*), which uses a methodology also developed in Ser-Giacomi et al. (2015*a*) and Ser-Giacomi et al. (2015*b*). Here, the important point is to notice the difference between the transport characteristics of the upper and of the lower panel. In the first case trajectories become confined to the east and to the west of the area of study, whereas in the second panel some of the trajectories starting in the west cross towards the east side. We want to find indicators and precursors of this transition in the topology of the flow. In the real atmospheric system the change occurs in time. To have a more controlled test bench we analyze here an analytical flow system in which a similar transition occurs when a parameter changes.

The chosen model flow is the so-called double-gyre. See for example Shadden et al. (2005) or Farazmand and Haller (2012) for basic properties of this system and computations of its Lagrangian coherent structures and Lyapunov fields. The double-gyre is a two-dimensional time-periodic flow defined in the rectangular region of the plane

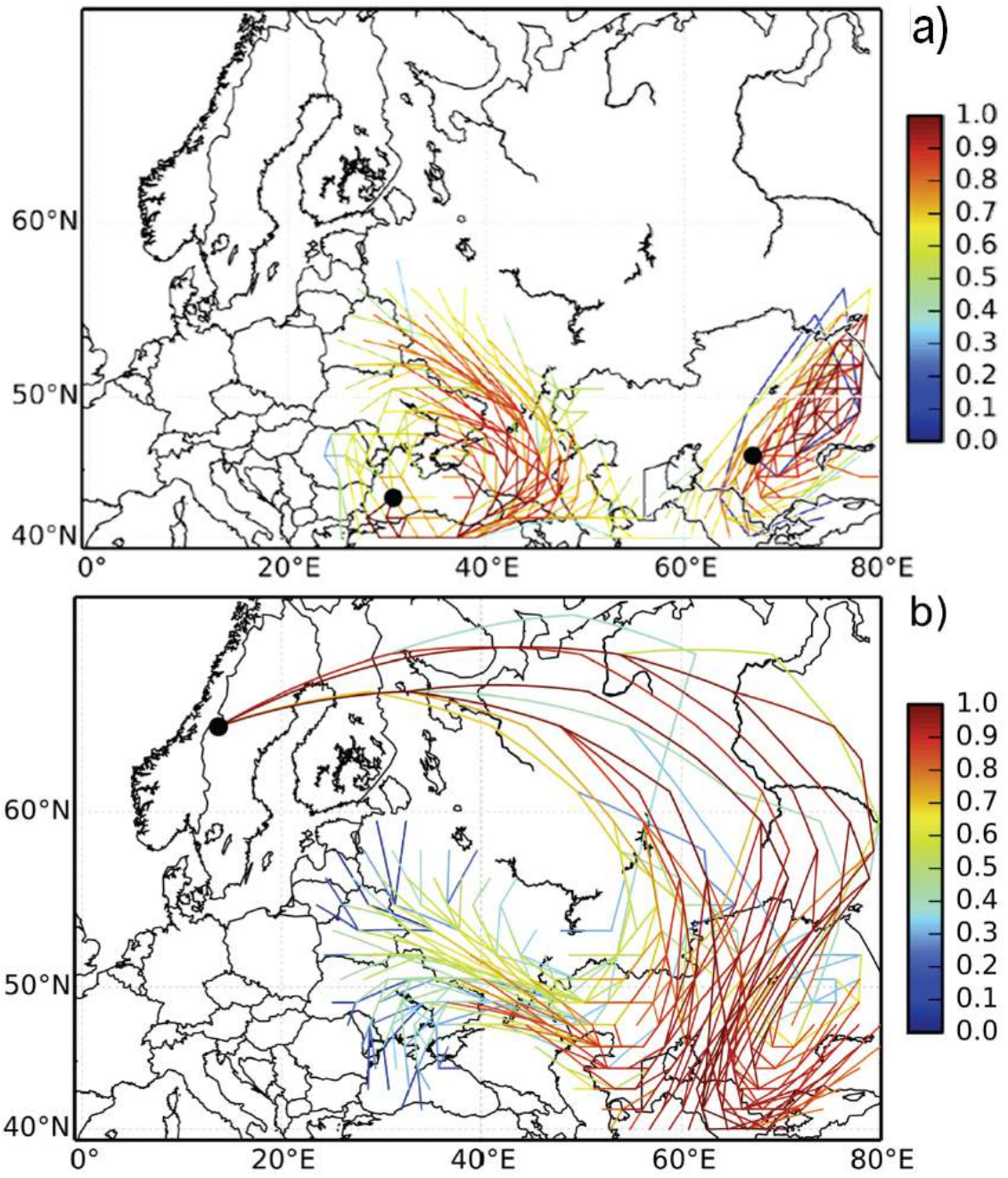

Figure 1: Discretized optimal paths of the air parcels released from the solid circles during the locking event in July 2010. Colors indicate the paths's probabilities in normalized logarithmic scale. Two different flow regimes are illustrated here: In the upper panel paths remain confined to the east and west regions, whereas transport from west to east occurs in the situation depicted in the lower panel.

$\mathbf{x} = (x, y) \in [0, 2] \times [0, 1]$. It is described by the streamfunction

$$\psi(x, y, t) = A \sin(\pi f(x, t)) \sin(\pi y) \, , \tag{1}$$

with

$$\begin{aligned} f(x, t) &= a(t)x^2 + b(t)x & (2)\\ a(t) &= \epsilon \sin(\omega t) \, , & (3)\\ b(t) &= 1 - 2\epsilon \sin(\omega t) \, . & (4) \end{aligned}$$

From these expressions, the velocity field (v_x, v_y) is

$$\begin{aligned} \dot{x} &= v_x = -\frac{\partial \psi}{\partial y} = -\pi A \sin(\pi f(x, t)) \cos(\pi y) & (5)\\ \dot{y} &= v_y = \frac{\partial \psi}{\partial x} = \pi A \cos(\pi f(x, t)) \sin(\pi y) \frac{\partial f(x, t)}{\partial x} \, . & (6) \end{aligned}$$

For $\epsilon = 0$, this flow is steady. Ideal fluid particles follow very simple trajectories: they rotate following closed streamlines, clockwise in the left half of the rectangle, and counterclockwise in the right one. The central streamline $x = 1$, a heteroclinic connection between the hyperbolic point at $(1, 1)$ and the one at $(1, 0)$, acts as a separatrix between the two regions. When $\epsilon > 0$, more complex behavior including chaotic trajectories arises. The periodic perturbation breaks the separatrix, so that now some interchange of fluid is possible between the left and the right part of the rectangle. The geometric structures involved in this interchange have been studied with a variety of techniques (Shadden et al., 2005; Farazmand and Haller, 2012) but the framework of optimal paths developed with the help of novel network methodologies (Ser-Giacomi et al., 2015*b*,*c*) seems quite natural for this purpose.

In Figs. 2 and 3, and in the rest of the paper, we take the parameters $A = 0.1$ and $\omega = 2\pi/5$. Then, we compute trajectory paths in our network framework for two qualitatively different situations, namely the steady case $\epsilon = 0$, and the periodically perturbed case (of period $2\pi/\omega = 5$) with $\epsilon = 0.3$. We discretize the fluid domain into $200 \times 100 = 20000$ square boxes, defining the nodes in our flow network, and compute the adjacency matrices of the Lagrangian network by releasing 400 particles from each of the boxes (see details in Ser-Giacomi et al. (2015*c*)). In all the cases shown below we compute paths of $M = 6$ steps of duration $\tau = 1$, starting at $t_0 = 0$.

Figure 2 considers the steady flow ($\epsilon = 0$) and shows all optimal paths emanating from two particular initial nodes and reaching all nodes accessible from them after the 6 steps. We see the general clockwise and anticlockwise circulations at each side of the separatrix. The two halves of the domain remain isolated. This is the situation analogue to the atmospheric flow configuration displayed in the upper panel of Fig. 1.

Figure 3 shows optimal paths for the periodically perturbed flow ($\epsilon = 0.3$). The general clockwise and counterclockwise rotations still remain, but now there are pathways connecting the two halves of the domain. Note the strong divergence of close pathways when they approach the hyperbolic region at the bottom of the domain, and how is this geometric structure what allows transport of fluid between the two regions that were isolated in the steady case. This is clearly similar to the lower panel in the atmospheric case of Fig. 1.

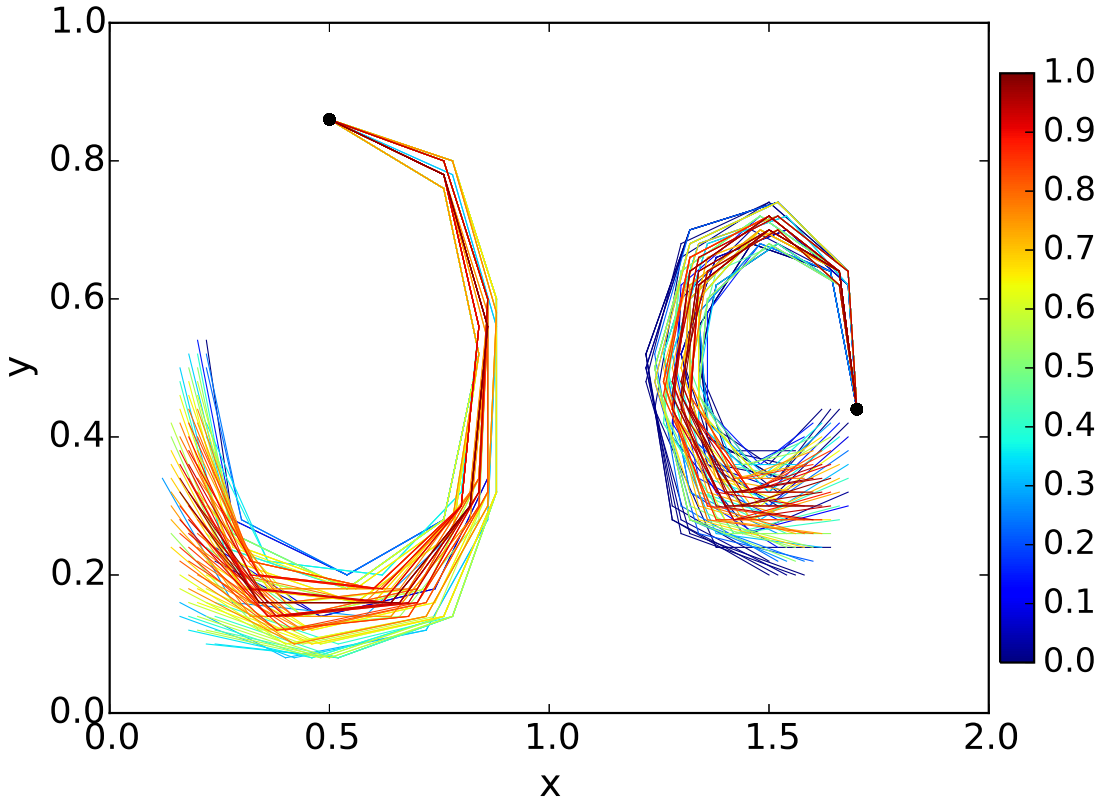

Figure 2: Double-gyre 6-step paths in the steady case $\epsilon = 0$, from two different starting nodes (the black circles) to all the accessible destinations. The network nodes pertaining to each path are joined by straight line segments colored according to the path probability. The color code is logarithmic in the full probability range, which is $[0.054, 7.73 \times 10^{-10}]$ for the left node (there is a total of 94 paths emanating from it) and $[0.0234, 10^{-7}]$ for the right one (87 paths).

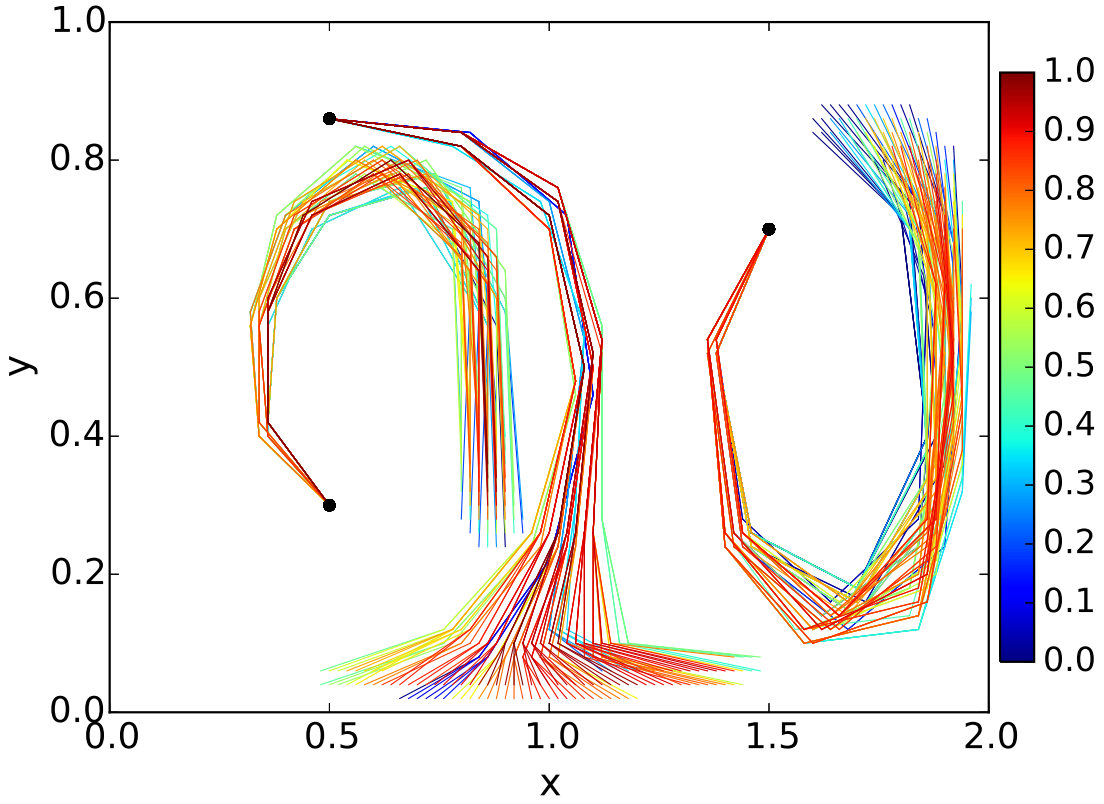

Figure 3: 6-step paths for the periodically perturbed double gyre at $\epsilon = 0.3$, from three different starting nodes (black circles) to all the accessible destinations. Color coding as in Fig. 2, with probability ranges which are $[0.0327, 3.355 \times 10^{-7}]$ (bottom-left node, 66 paths), $[0.0245, 1.879 \times 10^{-9}]$ (top-left node, 108 paths), and $[0.0128, 1.335 \times 10^{-8}]$ (right node, 106 paths).

3 Cross-flow transition

We now construct for the flow described in section 2 the corresponding flow network that describes the transport among the different nodes of the domain for full time lapse of $\tau = 6$ time units. To do this we use the methodology described in Ser-Giacomi et al. (2015*a*), Rossi et al. (2014), which is equivalent to the composition of the shorter-time networks constructed in Ser-Giacomi et al. (2015*b*) and Ser-Giacomi et al. (2015*c*). We are interested in the transition between a situation in which there is no flow between the left and the right part of the domain, and one in which transport occurs. Thus we define two subdomains $D_L = [x_1 = 0.05, x_2 = 0.95] \times [y_1, y_2]$ and $D_R = [x_1 = 1.05, x_2 = 1.95] \times [y_1, y_2]$, the *left* and the *right* domains, and compute the *cross-flow* among them, defined as the sum of all weights of links connecting nodes in D_L with nodes in D_R, in any direction.

Blue lines in the two panels of Fig. 4 give the cross-flow as a function of the parameter ϵ. We see that there is a transition between a situation at low ϵ in which there is no cross-flow between the two subdomains and a situation of non-vanishing cross-flow increasing with ϵ, starting at a critical value ϵ_c. The location of the transition, ϵ_c, depends on the geometry of the subdomains. D_L and D_R are larger for the panel on the left, so that the cross-flow between them starts at a lower value of ϵ, whereas a stronger chaotic mixing (larger ϵ) is needed to start cross-flow between the smaller domains corresponding to the right panel of Fig. 4.

4 Network indicators and discussion

We compute the following network indicators that have been demonstrated to be useful to locate and in some cases to anticipate regime changes in previously studied climatic networks (see Deliverables 5.2-5.4 and Van Der Mheen et al. (2013), Tirabassi et al. (2014) and Feng et al. (2014)). We apply them to the restricted flow network (treated as undirected and unweighted) in which only the nodes inside D_L and D_R are included. The indicators are:

- **Density of links**: it is the number of links present in the restricted network, normalized by the maximum possible number of links, i.e. $M(M-1)/2$, where M is the number of nodes in the restricted flow network.
- **Average clustering**: it is the number of closed triangles present in the restricted network, normalized by the maximum number of triangles which can be constructed with the given nodes.
- **Number of components**: the number of disjoint groups of connected nodes present in the network
- **C2**: The number of network components consisting exactly of two connected nodes. In this case components are only counted if the weight of the link joining their two nodes is larger than 0.33.

The behavior of these indicators as a function of ϵ, that eventually brings the network to a situation allowing cross-flow past a tipping point ϵ_c, is displayed also in Fig. 4.

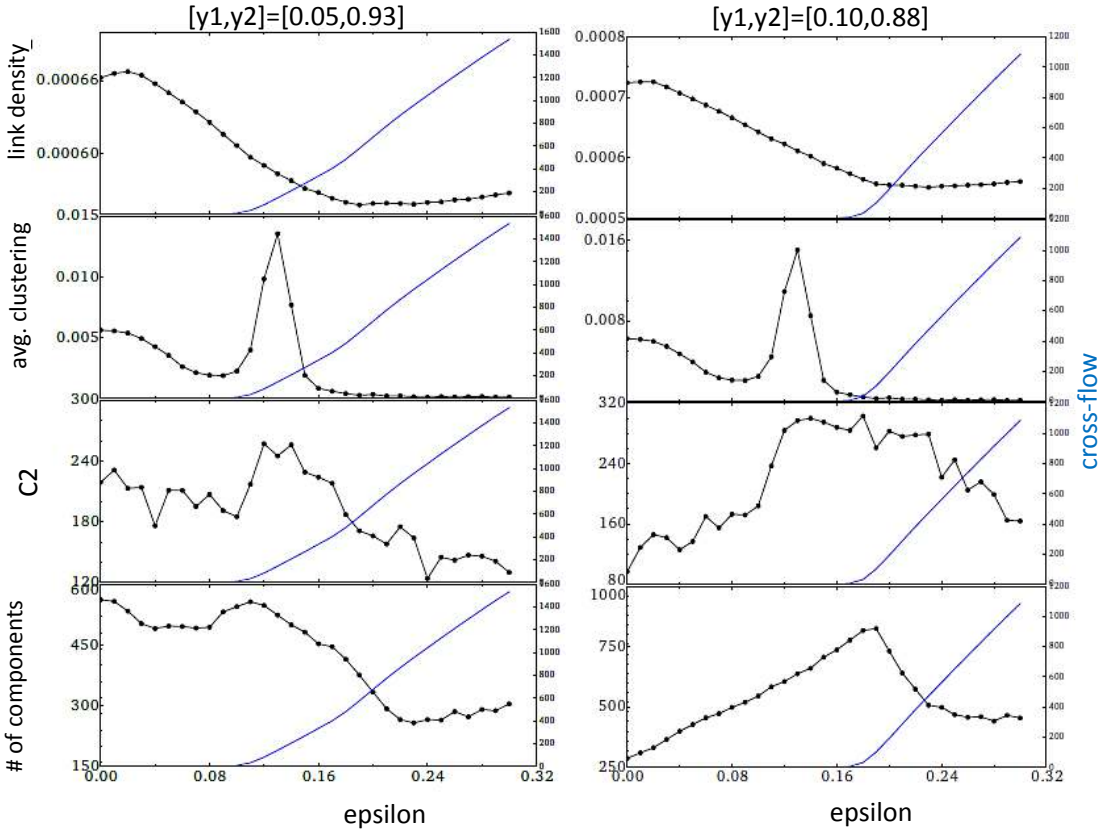

Figure 4: Different network indicators (black lines), compared with the cross-flow between left and right subdomains (blue lines). The left and right panels differ in the vertical extension $[y_y, y_2]$ of the considered subdomains D_R and D_L, as indicated in the figure. Subdomains are larger for the left panel.

Link density has a rather uninformative behavior. It mostly decays with increasing value of ϵ. The two component-based indicators, however, have a maximum value when the cross-flow transition occurs. The maximum is sharper when the cross-flow changes more abruptly. Thus, as in the case of climatic networks built from correlations, the number of components and the quantity $C2$ reflect the topological change in the transport network by taking a maximum value.

The most interesting behavior appears for the average clustering. There is a sharp and distinct peak for intermediate values of ϵ. We see that this maximum either coincides or occurs *before* the cross-transition happens. Thus, this quantity is a candidate to be taken into account *to anticipate* transitions. The location of the clustering peak sees to be the same independently of the size of the subdomains D_L and D_R (until they are so small that the network fully disconnects). Thus, it reflects an internal reorganization of the transport process at a local level, rather than the global result that arises from the different subdomain geometries. Probably the strong clustering appears just before the chaotic transition which destroys most of the KAM tori and barriers to transport, a local phenomenon that would anticipate the appearance of the large-scale transport characterized by the rise of the cross-flow. In consequence, clustering seems to be a good candidate to anticipate transport regime changes before actually reaching the tipping point.

Although the above is the most reasonable and promising hypothesis, we can not exclude that other mechanisms for the clustering peak, not directly related to transport transition, are at play. Analysis of additional model flows is required to further confirm the identification between the maximum in clustering and a precursor of the cross-flow transition.

In summary, the number of network components and the quantity $C2$ are proper indicators of the change of regime in the transport process occurring in the studied Lagrangian flow network. The average clustering appears as a very promising early warning indicator, to which further study should be devoted.

References

Mohammad Farazmand and George Haller. Computing Lagrangian coherent structures from their variational theory. *Chaos* 22(1), 013128 (2012).

Qing Yi Feng, Jan P. Viebahn, and Henk A. Dijkstra. Deep ocean early warning signals of an atlantic moc collapse. *Geophysical Research Letters* 41(16), 6009–6015 (2014).

Vincent Rossi, Enrico Ser-Giacomi, Cristóbal López, and Emilio Hernández-García. Hydrodynamic provinces and oceanic connectivity from a transport network help designing marine reserves. *Geophysical Research Letters* 41(8), 2883–2891 (2014).

Enrico Ser-Giacomi, Vincent Rossi, Cristóbal López, and Emilio Hernández-García. Flow networks: A characterization of geophysical fluid transport. *Chaos* 25, 036404 (2015*a*).

Enrico Ser-Giacomi, Ruggero Vasile, Emilio Hernández-García, and Cristóbal López. Most probable paths in temporal weighted networks: An application to ocean transport. *Physical Review E* 92, 012818 (2015*b*).

Enrico Ser-Giacomi, Ruggero Vasile, Irene Recuerda, Emilio Hernández-García, and Cristóbal López. Dominant transport pathways in an atmospheric blocking event. *Chaos* 25, 087413 (2015*c*).

Shawn C. Shadden, Francois Lekien, and Jerrold E. Marsden. Definition and properties of Lagrangian coherent structures from finite-time Lyapunov exponents in two-dimensional aperiodic flows. *Physica D* 212(34), 271–304 (2005).

G. Tirabassi, J. Viebahn, V. Dakos, H.A. Dijkstra, C. Masoller, M. Rietkerk, and S.C. Dekker. Interaction network based early-warning indicators of vegetation transitions. *Ecological Complexity* 19, 148 – 157 (2014).

Mirjam Van Der Mheen, Henk A. Dijkstra, Avi Gozolchiani, Matthijs Den Toom, Qingyi Feng, Jürgen Kurths, and Emilio Hernandez-Garcia. Interaction network based early warning indicators for the atlantic moc collapse. *Geophysical Research Letters* 40(11), 2714–2719 (2013).